

Difference between the effects of modification graphene oxide with two biomass molecules: Chitosan and cardanol

Guomei Xu · Tiejun Shi · Ming Li · Fu Yu ·
Ying Chen

Received: 18 October 2014 / Accepted: 18 December 2014 / Published online: 13 January 2015
© Springer Science+Business Media Dordrecht 2015

Abstract To improve the dispersion of graphene oxide (GO) in a polymer matrix, two kinds of biomass molecules, chitosan (CS) and cardanol, were chosen to modify GO. CS and cardanol was mixed with GO in ethanol and agitation, respectively. The chain of CS was grafted onto GO, which were called KGO at here; cardanol chain were grafted onto GO and were called YGO in this paper. The chemical structures of KGO and YGO were characterized by FT-IR, TEM, respectively. The XPS results demonstrated that 40 % oxygen and 60 % carbon existed on the surface of GO. However, the elements content on the GO surface was altered after modification; 7.58 % nitrogen, 26.16 % oxygen, and 63.05 % carbon were observed on the surface of KGO. Furthermore, 93.85 % carbon and 6.15 % oxygen existed on the surface of YGO. The curing behavior of GO was characterized by DSC. There was only one exothermic peak around 172 °C during cure. Compared with the DSC curve of GO, one endothermic peak around 105 °C and two exothermic peaks at 224 and 310 °C were found during the cure of KGO; two exothermic peaks around 160 and 310 °C appeared during the curing of YGO. The thermal stability was studied by TGA. The TGA curves of KGO and YGO all showed three stages during the degradation, which were different from a linear degradation during GO. The fracture properties of GO after modification were also characterized by FESEM in this paper.

G. Xu · T. Shi (✉) · M. Li · F. Yu · Y. Chen
School of Chemistry and Chemical Engineering of Hefei University of Technology,
Hefei 230009, People's Republic of China
e-mail: stjhfut@163.com

G. Xu
School of Materials and Chemical Engineering of West Anhui University,
Lu'an 237012, Anhui, People's Republic of China

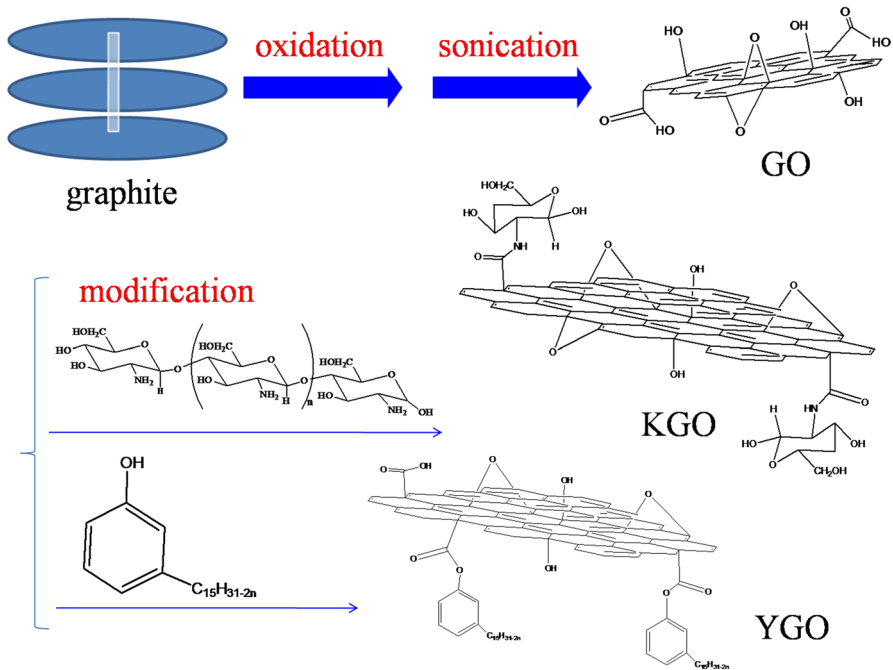
Keywords Biomaterial · Graft and mixing · Agitation · Ethanol · Environmental preservation

Introduction

Graphene, a two-dimensional carbon material, is prepared from graphite carbon by mechanical exfoliation ('Scotch-tape') method and epitaxial chemical vapor deposition [1]. Graphene offers unique intriguing and unparalleled properties, which show potential application in wastewater treatment [2], biological sensors, lubricants, and so on [3]. However, it is difficult to obtain perfect single graphene sheets in practical application, and many researchers have found that there is an effective way to prepare graphene by reducing GO. GO could be made by chemical oxidization of graphite, thus multiple oxygen groups such as epoxide, hydroxyl, and carboxyl could be attached on the surface [4]. These functional oxygen groups ensure GO good hydrophilicity [5]. Considerable work has been made on graphene and GO sheets recently owing to their unique electronic, chemical, and mechanical properties [6]. A wide application of graphene and GO is by dispersing them in a polymer matrix as a reinforcement of polymer composites [7]. However, graphene and GO sheets tend to aggregate in the composites severely, which constrains their application [8]. So far, functionalized graphene-based materials through chemical grafting have been suggested as an efficient approach to improving the compatibility among the sheets and polymer matrix [9]. The surface covalent modification to optimize the physical and chemical properties of GO or graphene sheets, so as to facilitate the interfacial adhesions between polymer and sheet, and also to broaden their applications [10]. For example, Deng et al. [11] reported functionalized graphene sheets with pre-synthesized polymer, offered graphene could be easily dispersible in organic solvents. Zheng et al. [12] modified GO flakes with cationic surfactant cetyltrimethylammonium bromide (CTAB) and prepared macroporous polymer–GO composites by Pickering emulsions. Kuila et al. [13] prepared functionalized graphene with sulfonated poly (ether–ether–ketone) (SPEEK) and used as a supercapacitor electrode for a green energy storage system.

Currently, technological developments aiming at the production and usage of new materials derived from renewable organic raw materials as starting materials are attracting the attention of both academic and industrial researchers. Using biomaterials to modify GO could be a new possible method due to its no or less toxicity and health-related issues [14].

Chitosan (poly- β -(1 \rightarrow 4)-2-amino-2-deoxy-D-glucose, CS) is a biodegradable polyaminosaccharide that comes from the *N*-deacetylated derivative of chitin [15]. The structure of CS is shown in Scheme 1. Recently, great attention has been paid to CS as a biological active resource [16]. Omura et al. [17] have recently reported the synthesis of chitosan-based benzoxazine from CS and phenol. The reaction was treated with paraformaldehyde in a mixture of water and methanol (1:1). However, much attention has been paid to CS due to the great percentage of nitrogen (6.89 %) compared to synthetically substituted materials [18]. The most important was that the nitrogen atom in CS was mainly in the form of primary aliphatic amino groups that existed [19]. Therefore, CS could undergo *N*-acylation [20] and Schiff reactions, which were both typical reactions of amines [21] and all could be easily happened under mild condition [22].



Scheme 1 Preparation of KGO and YGO

Cardanol is obtained from vacuum distillation cashew nut oil [23]. As reported in the literature, cardanol is a mixture of phenol. There would be 3-*n*-pentadecylphenol, 3-(pentadeca-8-enyl) phenol, 3-(pentadeca-8,11-dienyl) phenol, and 3-(pentadeca-8,11,14-trienyl) phenol. Considerable work [24] has proven that the long alkyl chain *meta* substitution of the phenolic ring offers attractive properties to cardanol [25].

The purpose of this article is to discuss the effects of modification GO with CS and cardanol, grafting *O*-substituted glucans on GO; we called it KGO; grafting cardanol chain on GO, which was named YGO later. Then the difference between the surface structure and thermal properties of KGO and YGO was described in this paper. The surface characteristics of KGO and YGO were studied by XPS and TEM. The thermal properties were measured by TGA and compared to each other to further understand the role of these two biomaterials after being grafted onto the GO surface. The FESEM images of KGO, YGO, and GO were discussed, and its modification mechanism was also proposed.

Experimental

Materials

Cardanol was obtained from Shangdong Haobo Biological Materials Co., Ltd. $M = 304.52$; CS was bought from Shanxi Sciphar Hi-tech Industry Co., Ltd; Graphite flakes were kindly supported by Hefei General Machinery Research Institute.

Hydrogen peroxide (30 %), sulfuric acid (98 %), hydrochloric acid (37 %), concentrated phosphoric acid, and potassium permanganate, were purchased from Shanghai Zhengqi Chemical Reagent Co. Ltd (Shanghai, China). Deionized water was used in the entire work.

Preparation of GO

Oxidized graphite was prepared with graphite flake in our laboratory via improved Hummer's method [26]. The specific procedure was described as follows: 360 ml of sulfuric acid (98 %) and 40 ml of concentrated phosphoric acid were added slowly to a mixture of 3 g graphite flakes and 12 g potassium permanganate. Stirred the reaction for a few minutes till the temperature of the solution no changed, then heated up to 50 °C and continued stirred for 12 h. Subsequently, the reaction was quenched by adding 30 ml 30 wt% H₂O₂. The mixture was kept in an ice bath to cool. A viscosity solution was obtained and washed continuously with 100 ml 30 wt% hydrochloric acid and 100 ml of water three times. Oxidized graphite was filtered from the viscosity solution. Ultrasonication and centrifugation of the oxidized graphite, graphene oxide (GO), was achieved. GO was used with no any further work all through.

Preparation of KGO and YGO

Modification GO with CS was carried out by a facile way as shown in Scheme 1. We took 0.5 g of CS blended with 2 g of graphite oxide in 100 ml of alcohol solution and then added a drop of acetic acid to promote the reaction. After that sonicated for a few hours till uniform solution, then filtered to remove the lower precipitation, dried the product in vacuum at 60 °C for a day, black solid product was isolated, which was referred as KGO.

Modification of GO with cardanol was carried out as follows: We took 2 g of graphite oxide dispersed in 100 ml of alcohol and sonicated to a uniform solution, and then 0.5 g of cardanol was added, and then the mixture was stirred for 4 h at 80 °C. Follow on filtered and dried the product in vacuum at 60 °C for a day, black solid product was isolated, which was referred to as YGO.

Thermal curing of GO, KGO, and YGO

The GO, KGO, and YGO were all heated in a stainless-steel rectangular mold with a stepwise cure in an air-circulating oven. The curing procedure was executed as follows: 100 °C for 2 h, 120 °C for 2 h, 140 °C for 2 h, 180 °C for 2 h, 200 °C for 2 h, and 240 °C for 1 h.

Measurements

A field emission scanning electron microscope (FE-SEM) was used to observe the morphology of the samples on a FEI Sirion200 system operated at an accelerating voltage of 5 kV. Fourier transform infrared (FT-IR) spectra were recorded on a

spectrophotometer (Thermo Nicolet, Nicolet-6700) with potassium bromide as a reference. Differential scanning calorimetry (DSC) was employed at a heating rate of 10 °C/min in 200 ml/min nitrogen atmosphere to study the effect of biomaterials on the properties of GO on TA Q2000. The thermal stability and weight loss of samples were performed on thermogravimetric analysis (TGA) by TGA Q5000 (New Castle, DE) at a heating rate of 10 °C/min in a nitrogen atmosphere. The gas flow rate was 100 ml/min. An ultrasonic cleaning instrument was used to exfoliate graphite oxide in a KQ-100E sonicator (100 W). Field emission transmission electron microscope (FETEM) images were measured on a Hitachi SU8020 TEM. The surface atomic structures of samples were analyzed by X-ray photoelectron spectroscopy (XPS) on an ESCALAB 250 (Thermo-VG Scientific USA).

Results and discussion

Characterizations of GO after functionalization

FT-IR was used to analyze and identify the chemical structure of the substances. To verify that the chemical structure had changed after modification, the FT-IR spectra of GO, CS, cardanol, KGO, and YGO were also present in Fig. 1. To GO, the adsorption bands at 1,730 cm^{-1} correspond to the C=O carbonyl stretching and the adsorption bands at 1,226 and 1,065 cm^{-1} correspond to the C–O–C and C–O stretching, respectively [27]. A broad and intense signal at 3,413 cm^{-1} revealed the O–H stretches. The adsorption bands appearing at 1,628 cm^{-1} could be the skeletal vibrations of some unoxidized graphite. In comparison to the FT-IR spectra of KGO, besides the ubiquitous characterizations of GO, a signal of N–H vibration at 1,645 cm^{-1} appeared, which would be some $-\text{NH}_2$ groups on the CS had reacted

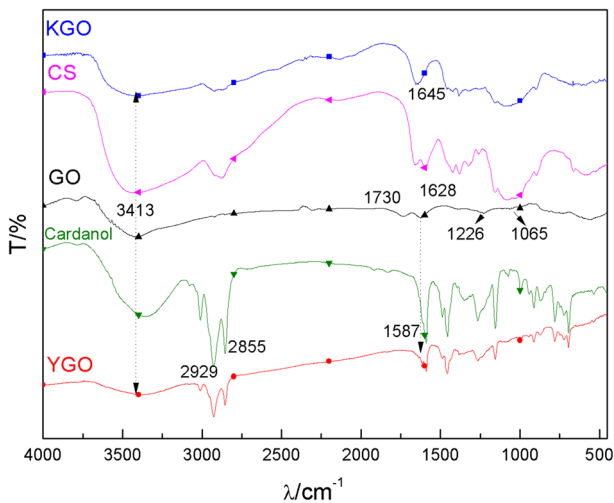


Fig. 1 FT-IR spectra of GO before and after modification

with the -COOH groups on the surfaces of GO and so converted to -NHCO- groups [28]. In addition to the FT-IR spectra of YGO, the resonance at $2,929$ and $2,855\text{ cm}^{-1}$ revealed the vibrations of -CH_2 and -CH [29] also appeared at the C=C adsorption bands at $1,587\text{ cm}^{-1}$, which all confirmed that some functional groups of CS and cardanol were grafted onto GO [30].

A field emission transmission electron microscope (FETEM) was employed to investigate the microstructure of the samples. The morphologies of GO were observed with a Hitachi SU8020 FETEM instrument. Exfoliated GO alcohol solution was deposited on a thin copper grid before observation. Figure 2 demonstrates that GO was successfully prepared from oxidized graphite. We could clearly see that the thin-sections attached to the copper mesh in Fig. 2a and no large particles were detected. Figure 2b shows that the effectively exfoliated GO sheets were nearly transparent. The edges of the suspended sheet tended to fold back, allowing for a cross-sectional view of the sheet with high resolution in Fig. 2c. In succession three or five layers could be found in Fig. 2d with more high resolution. Multi-layer nanosheets tended to re-stack to form some agglomerates, so some dark lines appeared, as shown in Fig. 2b.

Figure 3 shows TEM micrographs of two biological molecules functionalized with GO, on the top of it was micrographs of CS functionalized GO, at the bottom of it was TEM images of cardanol functionalized GO. We could clearly find that all these graphs were rather different from those of GO. There was a typical dark wrinkled structure in the image of KGO-a, further amplification to be found that many globular inclusion exist in graph of KGO-b, which could be clearly seen in that of KGO-c, all these differential would be due to the presence of substitute

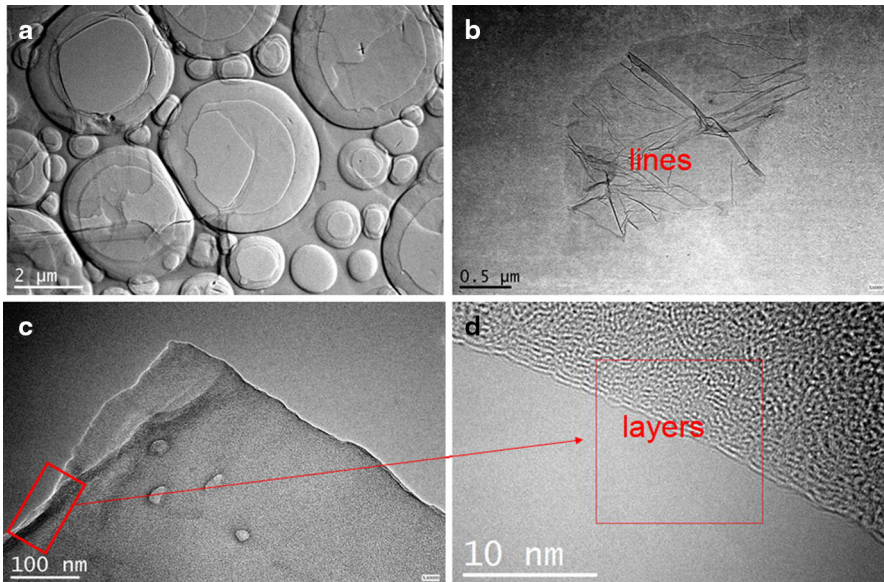


Fig. 2 FETEM images of well-exfoliated GO

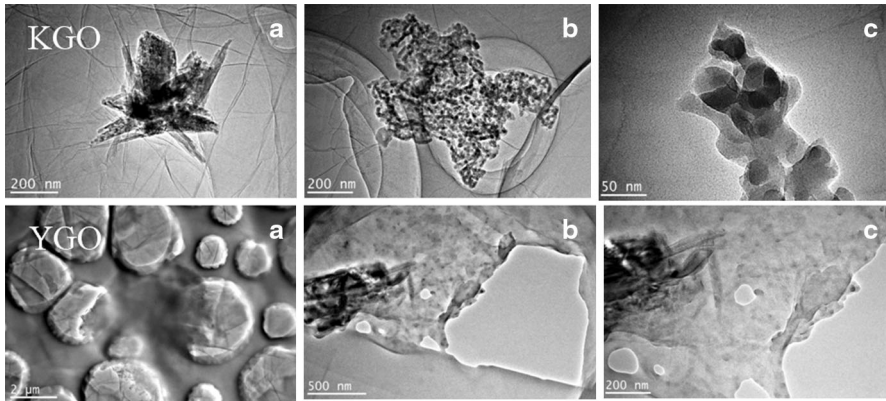


Fig. 3 FETEM images of modification of GO with cardanol and chitosan

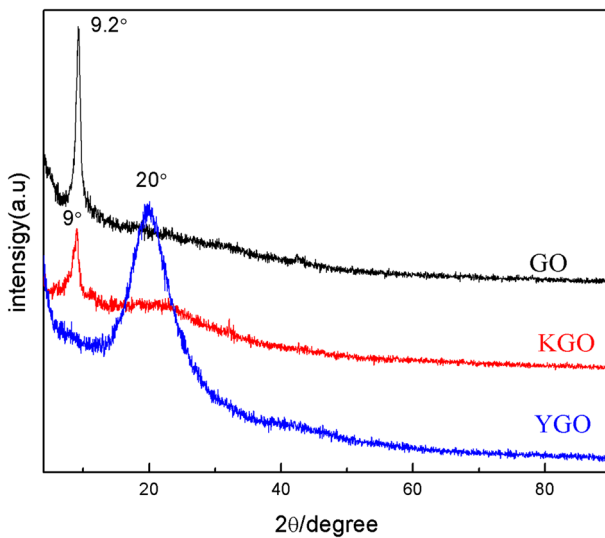


Fig. 4 XRD characterizations of GO, KGO, and YGO

glucans between layers after covalent functionalization. TEM images of YGO were present at the bottom of Fig. 3, which displayed cardanol functionalized GO, and it could be observed that there became not transparent in YGO-a when GO was functionalized with cardanol, which due to cardanol was extracted from the cashew nut shell oil, part oil residual not to volatile all through. Following this, we observed through high magnification that it could be seen that many particles attached on the surface of the GO sheets, as shown in Fig. 3 (YGO-b, YGO-c). All of these micrographs indicated successful modification [31].

Structural changes were also characterized by XRD spectra. The XRD pattern of GO was presented for comparison with two biological molecules functionalized GO, which are all shown in Fig. 4. The specific reflection peak of GO appeared at

$2\theta = 9.2^\circ$. These values of 2θ are similar to those reported in the literature [8, 26]. The diffraction angle of functionalized GO with CS appeared at $2\theta = 9^\circ$. The smaller values of 2θ indicated that the interlayer distance increased, which could be attributed to the amine and hydroxyl groups of CS. All these groups could react with *O*-containing functional groups of GO and further exfoliate the flakes of GO. However, the XRD pattern of YGO showed a higher value of 2θ at 20° relative to GO. This effect would be due to the long unsaturated aliphatic chain of cardanol adsorbed on the surface of GO, decreased the hydrophilic of GO sheets dramatically and made them aggregated.

XPS spectra were analyzed to determine the surface chemical composition of the materials and to further identify the above statement [32]. Figure 5 shows the XPS spectra of original GO. The ration of C1s and O1s in Fig. 5a demonstrated that there were many *O*-containing functional groups existing on the GO surface, and furthermore found that there were five different chemically shifted components that existed in C1s core level spectra: $sp^2C=C$ (~ 284.4 eV), $sp^3 C-C$ (~ 284.8 eV), $C-OH$ (~ 285.3 eV), $C=O$ (~ 287.1 eV), $C(=O)O$ (~ 288.6 eV), which are clearly present in Fig. 5c. O1s spectra was also resolved the overlapping peaks and found three different functional groups: $O-H$ (~ 531.7 eV), $O-C$ (~ 532.7 eV), $O=C-O$ (~ 533.3 eV). After being functionalized, although KGO and YGO both showed photoemission peaks for C1s (~ 285 eV) and O1s (~ 532.0 eV), the intensity of the peaks was changed. O1s photoemission peaks of KGO were much stronger than that

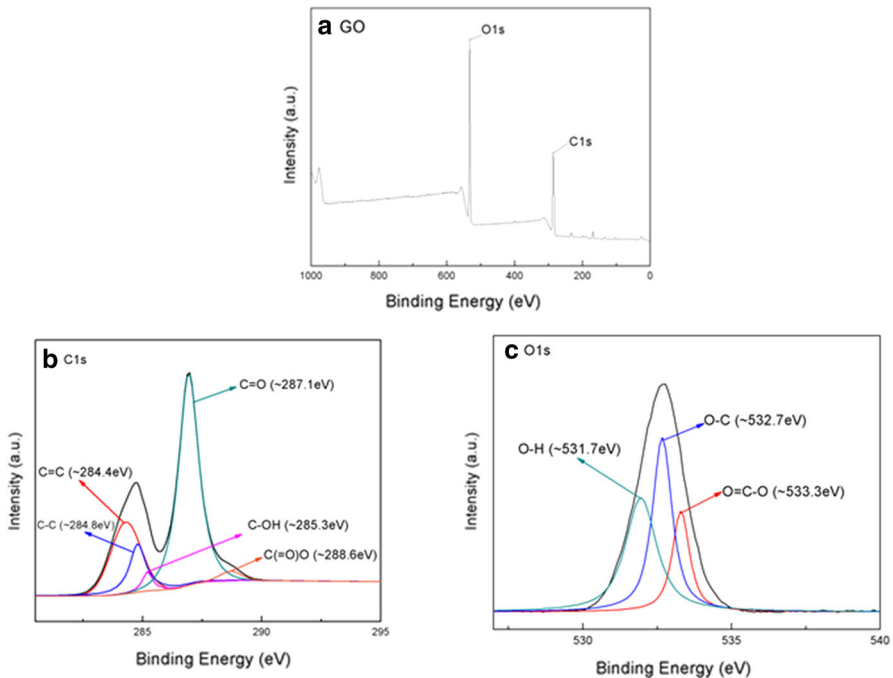


Fig. 5 XPS spectra of GO (a) C1s XPS spectra of GO (b), and O1s XPS spectra of GO (c)

of YGO, and N1s photoemission peaks (~ 398.4 eV) were only examined in KGO spectra. This phenomenon is due to the fact that the CS chains possess a high ratio of C–OH, C–O and $-\text{CH}_2-\text{NH}_2$ in their molecular structure. Six significant contributions were identified in the C1s core level spectra of KGO in Fig. 6c. Besides the detailed C1s XPS spectra as mentioned in GO, carbon atoms with a binding energy of ~ 286.8 eV also appeared corresponding to amide groups (C–N), carbon atoms with a binding energy of ~ 288.4 eV were attributed to oxygen carbonyl groups C(=O)O. N1s spectra were identified in Fig. 6b. Three significant contributions were found, corresponding to the values reported in the literature [33]: CH_2-NH_2 (~ 399.1 eV), N–C=O (~ 400.2 eV), $\text{CH}_2-\text{NH}-\text{CH}_2$ (~ 401.1 eV). The presence of amide carbonyl groups N–C=O (~ 400.2 eV) in KGO, which confirmed that the covalent attachment of CS chain on GO surface was succeed, so appeared amide carbonyl groups in KGO. The C1s core level spectra of YGO are shown in Fig. 7b. YGO exhibited four different chemically shifted components: $\text{sp}^2\text{C}=\text{C}$ (~ 284.4 eV), $\text{sp}^3\text{C}-\text{C}$ (~ 284.8 eV), C–OH (~ 285.5 eV), C–O–C (~ 286.2 eV), which implying the long hydrocarbon chain of cardanol grafted on GO surface, so the content of carbon increased in YGO. The specific element content is listed in Table 1.

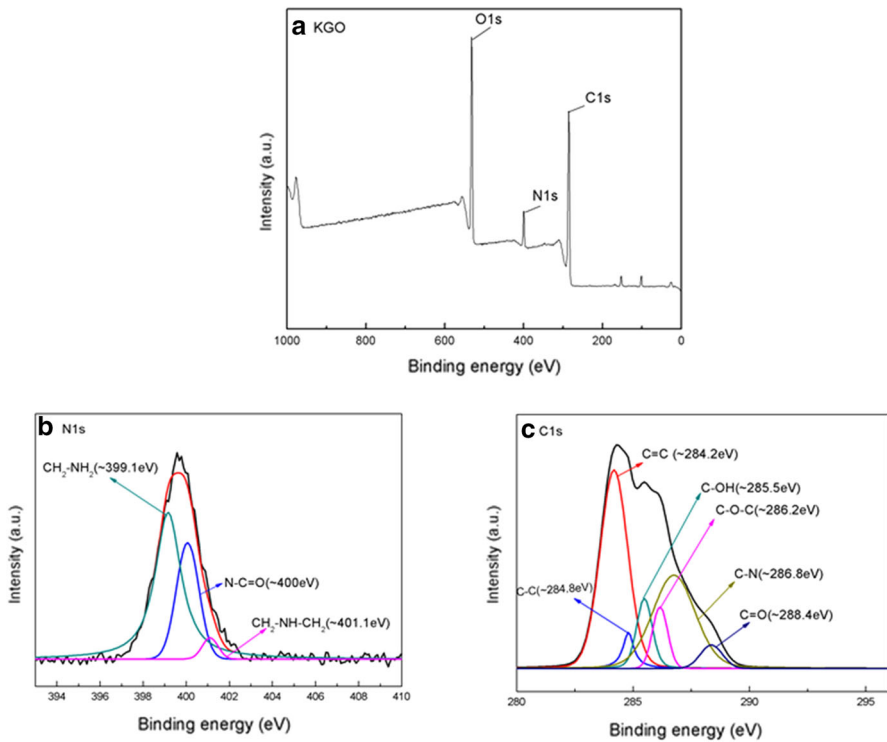


Fig. 6 XPS spectra of KGO (a), N1s XPS spectra of KGO (b), and C1s XPS spectra of KGO (c)

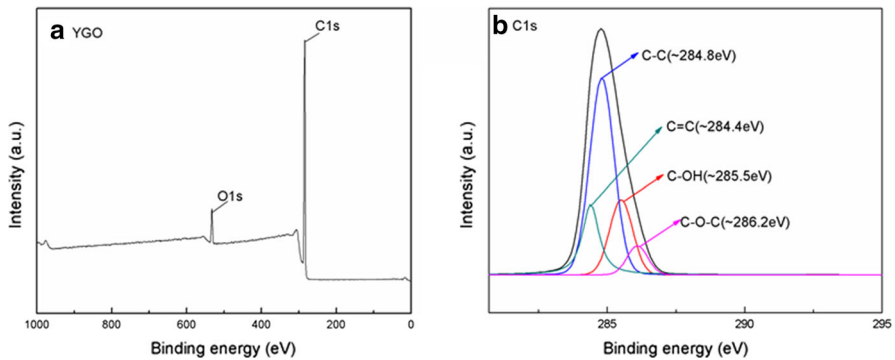


Fig. 7 XPS spectra of YGO (a) and C1s XPS spectra of YGO (b)

Table 1 Element contents of GO, KGO, and YGO

Samples	Element analysis on the surface (wt%)		
	C	O	N
GO	60	40	0
KGO	63.05	29.37	7.58
YGO	93.85	6.15	0

Thermal stabilities of GO, KGO, and YGO

For further investigated characterizes of functionalized GO, DSC was employed to analyze the effect of CS and cardanol during the curing behavior of GO. The results are shown in Fig. 8. The DSC curve of GO had one small endothermic peak below 100 °C and one strong exothermic peak around 172 °C. The endothermic reaction is due to residual water by *O*-containing functional groups on GO sheets that need to absorb thermal during the curing. The exothermic reaction attributed to decomposition of many containing oxygen functional groups from GO surface, such as hydroxyl and carbonyl groups. After functionalizing GO with CS, three obvious peaks were obtained, including one endothermic peak and two exothermic peaks. The first was an endothermic peak around 80 °C would be due to the residual of CS particles melting, the second was an exothermic peak around 224 °C, which corresponded to the fracture of many *O*-containing functional groups from GO surface, just for CS functionalized GO the curing behavior changed, the cure temperature increased, which displayed the thermal properties became stable than pure GO. The last was also a strong exothermic peak at 310 °C, which corresponded to the decomposition of attached CS chain on GO, which showed GO was functionalized successfully. By comparison, the thermal stability of GO also became better after being functionalized with cardanol. There were two exothermic peaks during the curing of YGO, the temperature of many hydroxyl and carbonyl groups ruptured from GO surface became higher than original GO appeared at 160 °C, and the other exothermic temperature appeared at 310 °C corresponded

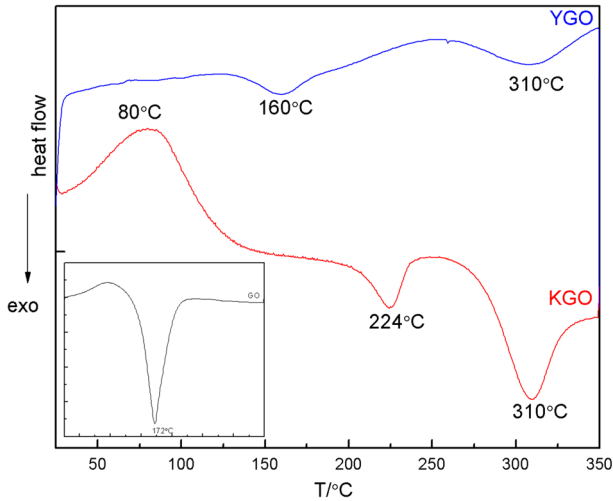


Fig. 8 DSC curves of GO, KGO, and YGO

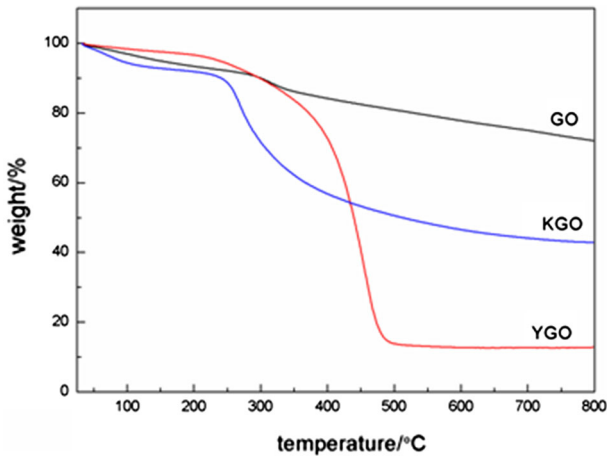


Fig. 9 TGA curves of GO, KGO, and YGO

with the removal of cardanol attached on GO. These effects demonstrated that the curing behavior of GO changed after modification with CS and cardanol [34].

The thermal stability of GO, KGO, and YGO were also analyzed by TGA after being cured and the results are shown in Fig. 9. Their thermal degradation was different from each other [35]. GO lasted for degradation during the whole process. The weight loss of GO began as soon as it was heated and 72 % char yield was obtained at 800 °C. A dramatic weight loss was shown before 300 °C, which was due to the decomposition of hydroxyl; epoxide, diol, ketone, and carboxyl functional groups on GO surface. This phenomenon corresponded to the results in

Table 2 Decomposition temperatures of GO, KGO, and YGO

Samples	$T_{\max}/^{\circ}\text{C}$	$T_5/^{\circ}\text{C}$	$T_{10}/^{\circ}\text{C}$	Char yield/%
GO	315	149	300	72
KGO	277	100	240	42.9
YGO	456	239	300	12.8

Fig. 7. As seen from the thermal degradation curve of functionalized GO, there were all smooth relative to pure GO. The mainly mass decomposing ranged from 300 to 500 °C, which was due to the amount of oxygen functional groups on GO surfaces decreased. Among the thermal degradation of KGO appeared three stages. The first scope was below 100 °C, in which the weight loss was caused by the residual CS molecules. The second region was from 100 to 290 °C, which can be attributed to the degradation of many labile oxygen functional groups, such as carboxylate, anhydride, and lactone groups. The third region started after 290 °C, in which the rate of weight loss became slow; obtain 42.9 % residual at 800 °C, which was attributed to the pyrolysis of CS moieties on GO sheets. Similar to KGO, there existed three ranges of weight loss of YGO. However, the tendency of thermal degradation of YGO was completely different from that of GO and KGO. There was nearly no weight loss below 200 °C. When the temperature increased to 500 °C, the weight loss of YGO kept no longer changed and obtained 12.8 % residual. Further, to compare the difference between GO modification, data related to the temperature corresponding to 5 wt% (T_5), 10 wt% (T_{10}) weight loss of the initial weight and T_{\max} weight loss (T_{\max}), as well as residues at 800 °C are listed in Table 2.

FESEM images of GO after functionalization

To describe the morphology of GO after functionalization, the fracture surface of samples was examined with a field emission scanning electron microscope (FESEM) [36]. The micrographs of graphite and GO were presence for comparison, which are shown in Fig. 10. The FESEM images of KGO and YGO are shown in Fig. 11. There was a significant difference between the micrographs of GO and functionalized GO. The modification effect was in a good agreement with TEM analysis. The images of graphite showed a bulky flake-like structure with smooth face. After oxidation and ultrasonication, the micrographs of pure GO showed a completely difference structure; the large flake-like structure disappeared and displayed a sheet-like structure with wrinkled edges, which demonstrated that GO was more exfoliated from graphite oxide. It was noted that the fracture surface of KGO displayed many wrinkled and thin crumble sheets. This effect was due to the chemical groups of CS being grafted on the GO surface, which corresponded to the TEM micrographs of KGO. However, the FESEM micrograph of YGO displayed a large thickness and also partial aggregation of GO. The fracture surface of YGO showed good lamellar and great thickness structure (marked as the red pane in Fig. 11). This is due to the phenolic hydroxyl group in cardanol reacted with *O*-

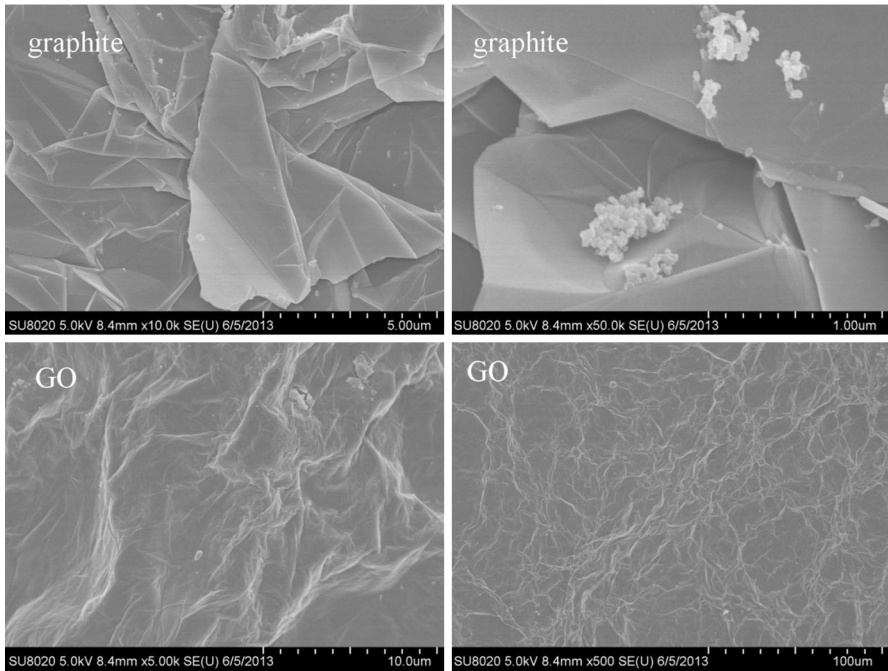


Fig. 10 FESEM micrographs images of graphite and GO

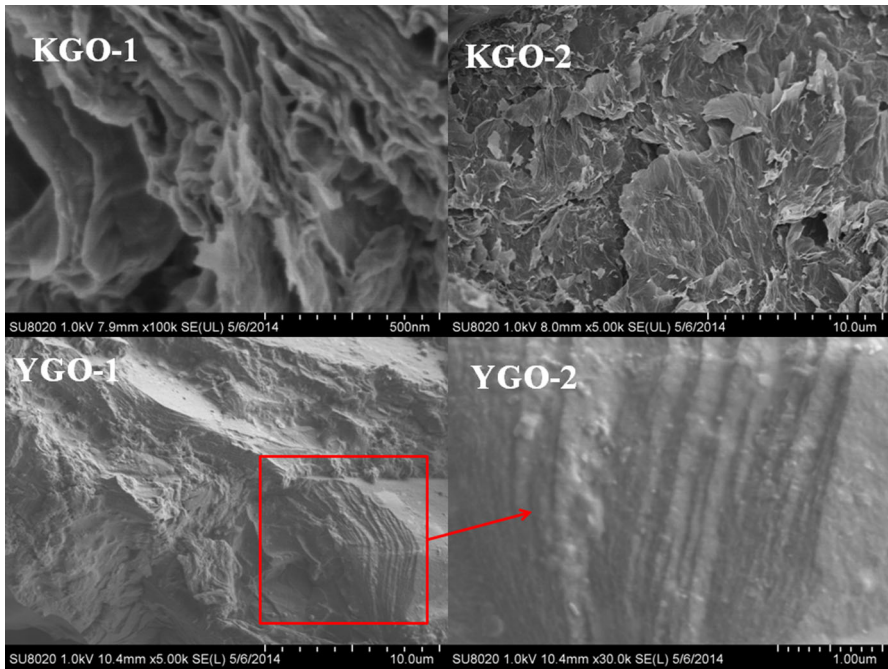


Fig. 11 FESEM micrographs images of KGO and YGO

containing functional groups of GO, the long side chain of cardanol increased the hydrophobicity of GO, caused GO restack and so increased the thickness of layers [37].

Conclusions

Two safe nontoxic biomass molecules (CS and cardanol) were used to modification GO generated two functionalized GO: KGO and YGO. The surface element content was examined with XPS and showed that there was 7.58 % nitrogen, 26.16 % oxygen, and 63.05 % carbon on the KGO surface and further investigation found nitrogen amide and carbon carboxyl groups all existed in KGO, which demonstrated that CS was grafted successfully on GO surface. The all characteristic of YGO confirmed that the long hydrocarbon chain of cardanol grafted on GO surface made the hydrophobic of GO changed and caused GO reunite. The micrographs of TEM and FESEM all showed that GO was successfully modified with CS and cardanol. The results of TGA showed the thermal of KGO and YGO were more stable than pristine GO. These functionalized GO would be used in the polymer matrix in future.

Acknowledgments This research received financial support from the National Natural Science Foundation of China (Grant No. 51273054), partial support from Lu'an municipal research projects directional commissioned to West Anhui University (Grant No. 2013LWA014), and further partial support from the Key Laboratory of Biomimetic Sensor and Detection Technology of AnHui, Lu'an in China and Engineering Technology Center of Fine Chemicals Engineering of AnHui, Lu'an in China.

References

1. U.N. Maiti, W.J. Lee, J.M. Lee, Y. Oh, J.Y. Kim, J.E. Kim, J. Shim, T.H. Han, S.O. Kim, *Adv. Mater.* **26**, 40 (2014)
2. A.A. Alhwaige, T. Agag, H. Ishida, S. Qutubuddin, *RSC Adv.* **3**, 16011 (2013)
3. D. Berman, A. Erdemir, A.V. Sumant, *Mater. Today* **17**, 31 (2014)
4. L.R. Radovic, C. Mora-Vilches, A.J.A. Salgado-Casanova, *Chin. J. Catal.* **35**, 792 (2014)
5. P. Steurer, R. Wissert, R. Thomann, R. Mülhaupt, *Macromol. Rapid Commun.* **30**, 316 (2009)
6. H.W. Ha, A. Choudhury, T. Kamal, D.-H. Kim, S.-Y. Park, *ACS Appl. Mater. Interfaces* **4**, 4623 (2012)
7. W. Lei, W. Si, Y. Xu, Z. Gu, Q. Hao, *Microchim. Acta* **181**, 707 (2014)
8. Y. Jin, S. Huang, M. Zhang, M. Jia, D. Hu, *Appl. Surf. Sci.* **268**, 541 (2013)
9. C.R. Arza, H. Ishida, F.H.J. Maurer, *Macromolecules* **47**, 3685 (2014)
10. N. Zhang, H. Qiu, Y. Si, W. Wang, J. Gao, *Carbon* **49**, 827 (2011)
11. Y. Deng, Y. Li, J. Dai, M. Lang, X. Huang, *J. Polym. Sci. Polym. Chem.* **49**, 1582 (2011)
12. Z. Zheng, X. Zheng, H. Wang, Q. Du, *ACS Appl. Mater. Interfaces* **5**, 7974 (2013)
13. T. Kuila, A.K. Mishra, P. Khanra, N.H. Kim, M.E. Uddin, J.H. Lee, *Langmuir* **28**, 9825 (2012)
14. K. Bustos-Ramírez, A. Martínez-Hernández, G. Martínez-Barrera, M. Icaza, V. Castaño, C. Velasco-Santos, *Materials* **6**, 911 (2013)
15. V.S. Yeul, S.S. Rayalu, *J. Polym. Environ.* **21**, 606 (2012)
16. R. Meena, M.U. Chhatbar, K. Prasad, A.K. Siddhanta, *Carbohydr. Polym.* **83**, 1402 (2011)
17. Y. Omura, Y. Taruno, Y. Irisa, M. Morimoto, H. Saimoto, Y. Shigemasa, *Tetrahedron Lett.* **42**, 7273 (2001)
18. M.N.V.R. Kumar, *React. Funct. Polym.* **46**, 1 (2000)
19. D. Xu, K. Wu, Q. Zhang, H. Hu, K. Xi, Q. Chen, X. Yu, J. Chen, X. Jia, *Polymer* **51**, 1926 (2010)

20. S.S. Silva, S.M.C. Menezes, R.B. Garcia, *Eur. Polym. J.* **39**, 1515 (2003)
21. J. Yang, J.H. Yu, J.R. Strickler, W.-J. Chang, S. Gunasekaran, *Biosens. Bioelectron.* **47**, 530 (2013)
22. V.K. Yata, S.S. Ghosh, *Biotechnol. Lett.* **33**, 153 (2010)
23. G. Vasapollo, G. Mele, R. Del Sole, *Molecules* **16**, 6871 (2011)
24. E. Cal, A. Maffezzoli, G. Mele, F. Martina, S.E. Mazzetto, A. Tarzia, C. Stifani, *Green Chem.* **9**, 754 (2007)
25. B. Lochab, I.K. Varma, J. Bijwe, *J. Therm. Anal. Calorim.* **107**, 661 (2011)
26. D.C. Marcano, D.V. Kosynkin, J.M. Berlin, A. Sinitskii, Z. Sun, A. Slesarev, L.B. Alemany, W. Lu, J.M. Tour, *ACS Nano* **4**, 4806 (2010)
27. J. Yang, M. Wu, F. Chen, Z. Fei, M. Zhong, *J. Supercrit. Fluids* **56**, 201 (2011)
28. S. Mallakpour, A. Abdolmaleki, S. Borandeh, *Appl. Surf. Sci.* **307**, 533 (2014)
29. B.S. Rao, A. Palanisamy, *React. Funct. Polym.* **71**, 148 (2011)
30. S. Stankovich, R.D. Piner, S.T. Nguyen, R.S. Ruoff, *Carbon* **44**, 3342 (2006)
31. H. Ribeiro, W.M. Silva, M.-T.F. Rodrigues, J.C. Neves, R. Paniago, C. Fantini, H.D.R. Calado, L.M. Seara, G.G. Silva, *J. Mater. Sci.* **48**, 7883 (2013)
32. Y.J. Wan, L.C. Tang, L.X. Gong, D. Yan, Y.B. Li, L.B. Wu, J.X. Jiang, G.Q. Lai, *Carbon* **69**, 467 (2014)
33. H. Han, D. Pan, X. Wu, Q. Zhang, H. Zhang, *J. Mater. Sci.* **49**, 4796 (2014)
34. A.A. Alhwaige, T. Agag, H. Ishida, S. Qutubuddin, *Biomacromolecules* **14**, 1806 (2013)
35. S.N. Ariffin, H.N. Lim, F.A. Jumeri, M. Zobir, A.H. Abdullah, M. Ahmad, N.A. Ibrahim, N.M. Huang, P.S. Teo, K. Muthoosamy, I. Harrison, *Ceram. Int.* **40**, 6927 (2014)
36. J. Li, F. Wang, C.-Y. Liu, *J. Colloid Interface Sci.* **382**, 13 (2012)
37. Y. Lou, G. Liu, S. Liu, J. Shen, W. Jin, *Appl. Surf. Sci.* **307**, 631 (2014)